

Sedimentary responses to the Pleistocene climatic variations recorded in the South China Sea

Sébastien Boulay^{a,*}, Christophe Colin^a, Alain Trentesaux^b, Stéphane Clain^c,
Zhifei Liu^d, Christine Lauer-Leredde^e

^a *Intéractions et Dynamique des Environnements de Surface, UMR IDES-CNRS 8148, Bât. 504, Université Paris-Sud, 91405 Orsay Cedex, France*

^b *Processus et Bilans des Domaines Sédimentaires, UMR PBDS-CNRS 8110, Université Lille I, 59655 Villeneuve d'Ascq, France*

^c *Mathématiques Appliquées, CNRS-UMR 6620, Université Clermont II, 63117 Aubière, France*

^d *Marine Geology, Tongji University, Shanghai 200092, People's Republic of China*

^e *Dynamique de la Lithosphère, Université Montpellier II, 34095 Montpellier cedex 05, France*

Received 24 October 2006

Available online 11 May 2007

Abstract

Grain-size analyses, coupled with end-member modelling, have been performed on the terrigenous fraction of two Leg 184 Ocean Drilling Program sites (1144 and 1146) from the South China Sea. The grain-size distributions over the last 1.8 Ma enable a new interpretation of their connections to sea-level variations and East Asian monsoon strength. Previous investigations in this area have associated grain-size variability with enhanced eolian input during glacial stages. End-member modelling downgrades the importance of this eolian contribution and indicates that the sediments can be described as a mixture of three end-members: fluvial mud inputs, shelf reworking and river mouth migration. Grain-size variations in the Pleistocene section of the cores indicate a multiple-stage evolution: (i) from 1.8 to 1.25 Ma, the downcore grain-size variations are low but show a correspondence between monsoon rainfall intensity and the fine grain-sized fluvial inputs; no link with sea-level variations is noticeable; (ii) from 1.25 to 0.9 Ma, there is an increase (decrease) in the intermediate (fine) end-member (~ 100 kyr cycle) that is associated with the onset of a stronger summer monsoon and modest shelf reworking; (iii) from 0.9 to 0 Ma the grain-size record is dominated by global sea-level variations; each glacial stage is associated with extensive shelf reworking and conveyance of coarse particles to the basin.

© 2007 University of Washington. All rights reserved.

Keywords: South China Sea; Grain size; End-members modelling; East Asian monsoon; Mid-Pleistocene Transition

Introduction

The South China Sea is under the influence of the East Asian monsoon, characterized by seasonal switches in wind direction, precipitation and runoff (Webster, 1987). During winter months, a high-pressure cell over Asia induces cold and dry winds blowing from Central Asia to the North Pacific Ocean. Conversely, during summer months, the formation of a low-pressure cell over the continent induces a reversal in wind direction and heavy monsoon rainfall over most of Southeast Asia (Webster, 1987).

Past variability in East Asian winter monsoon strength have been intensively investigated in the Chinese Loess Plateau, North Pacific Ocean as well as South China Sea sediments. These studies indicate a strengthened winter monsoon during glacial marine isotope stages and enhanced summer monsoon during interglacial marine isotope stages. In most of these studies, winter monsoon strength variations are characterized by strong cyclicities at ~ 100 and 41 kyr with considerably smaller variance in the 23 kyr precession band, indicating a link between high-latitudes climatic changes and monsoon variations (e.g., An et al., 1990; Ding et al., 1995; Xiao et al., 1995; Wang et al., 1999; Jian et al., 2001; Beaufort et al., 2003). Recent studies have shown that the East Asian summer monsoon pattern could be independent from the winter monsoon intensity and be characterized by different orbital

* Corresponding author. Fax: +33 1 69 15 48 82.

E-mail address: boulay_sebastien@yahoo.fr (S. Boulay).

frequencies, which imply separate forcing controls. In the South China Sea terrigenous sediments records, a strong 23-kyr precession cycle has been observed in the East Asian summer monsoon intensity over the last 450 ka (Boulay et al., 2005), and during the period between 3.2 and 2.5 Ma (Wehausen and Brumsack, 2002). Dominant precession forcing of the summer monsoon has also been reported for the Indian monsoon system (Clemens et al., 1991; Colin et al., 1998, 1999).

The terrigenous-dominated cores examined here were drilled on the slope of the large northern shelf, in front of the Pearl River mouth (Fig. 1). This enables us to decipher a reliable record of paleoenvironmental variations affecting Southeast Asia, as well as to reconstruct the impact of the East Asian monsoon in this area (Wang et al., 1999; Wehausen et al., 2003; Liu et al., 2003; Sun et al., 2003; Tamburini et al., 2003; Wei et al., 2004; Boulay et al., 2005). On geological time-scales, changes in the summer or winter Asian monsoon strength potentially are an important factor driving erosion and weathering (e.g., Clift, 2006) of the surrounding land masses, as well as oceanic and atmospheric circulations.

One of the main objectives of this paper is to assess the different factors that may influence detrital input in the South

China Sea. The sedimentary record results from a complex mixture of parameters such as changes in sedimentary sources, specifically eolian or fluvial supply, combined with changes in land configuration or river mouth migration during sea-level oscillations. Unravelling the sedimentological and mineralogical records of inputs to the South China Sea by estimating the relative importance of each of these processes provides an exceptional archive for reconstructing past changes in East Asian summer and winter monsoon strength.

This paper presents grain-size analyses, combined with an inversion algorithm for end-member modelling of compositional data (Weltje, 1997), performed on Pleistocene sediments from Ocean Drilling Program (ODP) Sites 1144 and 1146 in the South China Sea (Fig. 1). This data set provides new insights into the significance of grain-size variability in the northern part of the basin. The methodology allows us to resolve the number of granulometric end-members (sub-populations) mixed within the sediment, and to assess the grain-size distributions of each sub-population as well as quantifying the proportion of each end-member through time. Each end-member may be related to two kinds of sediment processes: (1) mixing of sediment that is transported by independent mechanisms and/or supplied from

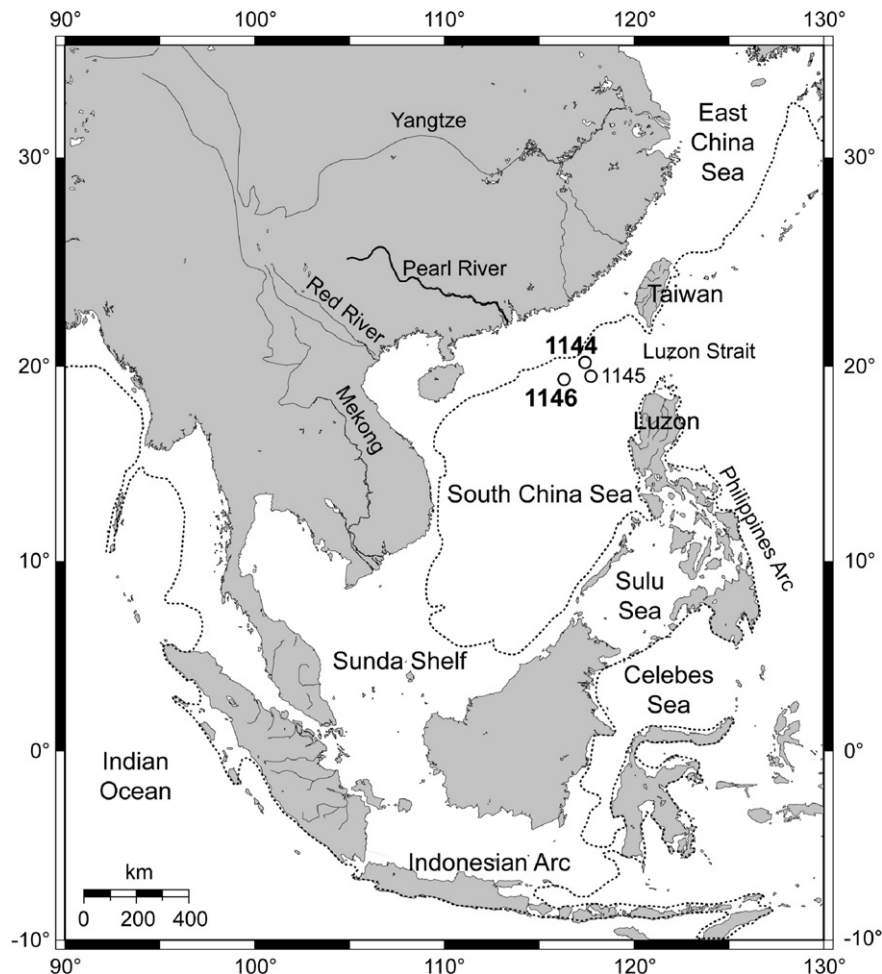


Figure 1. Localisation of the Ocean Drilling Program Sites 1144, 1145, 1146 in the northern margin of the South China Sea, in front of the Pearl River mouth. The dotted line shows the position of the shoreline during low sea-level stands as during the last glacial maximum (~120 m).

different sources and (2) selective mechanisms operating during unidirectional transport and deposition, producing sediment whose grain-size distributions change systematically with distance from the source. This method has already been successfully applied to grain-size distributions of Arabian Sea and North Atlantic sediments, and allows (depending on the site character) distinguishing between turbiditic, fluvial, eolian or ice-rafted sediments (e.g., Prins and Weltje, 1999; Prins et al., 2000). Utilizing this method, the grain-size record of both ODP Sites 1144 and 1146 can be translated in terms of sediment sources, transport dynamics (eolian, fluvial and/or oceanic supplies), as well as impact of Pleistocene climatic changes (East Asian monsoon intensity variations, glacial/interglacial sea-level changes and the Mid-Pleistocene Transition) on the detrital input to the South China Sea for the last 1.8 Ma.

Materials and methods

ODP Sites 1144 (20°03.18'N, 117°25.14'E; 2037 m water depth) and 1146 (19°27.49'N, 116°16.37'E; 2092 m water depth) are located in the northern part of the South China Sea, in front of the Pearl River mouth (Fig. 1). Age models for these drill cores were established using high-resolution planktonic and benthic foraminifera $\delta^{18}\text{O}$ records combined with biostratigraphic and magnetostratigraphic data (Clemens and Prell, 2003; Buehring et al., 2004). Core recovered at ODP Site 1144 extends for the last 1.1 Ma, with an average sedimentation rate of ~ 50 cm/kyr, while ODP Site 1146 has an average sedimentation rate of ~ 11 cm/kyr over the last 1.8 Ma. With the exception of five hiatuses observed in ODP Site 1144 during isotopic stages 5.5, 7.5–8, 9, 11 and 15, the sedimentary records of both sites are continuous (Clemens and Prell, 2003; Buehring et al., 2004).

Grain-size distribution measurements of ODP Site 1144 carbonate-free sediment were carried out on a Malvern Mastersizer X. Prior to analysis, bulk sediments were suspended in deionised water and gently shaken to achieve disaggregation. The suspension was then poured into the fluid module of the Mastersizer. After an initial analysis, hydrochloric acid in excess was added to the sample to obtain the grain-size distribution of the carbonate-free fraction. Using this method, the grain-size distributions of the carbonate-free fraction still include a marine opal component. ODP Site 1146 sediments were decarbonated by leaching with hydrochloric acid solution, then rinsed several times and centrifuged to eliminate the acid residue. The opal fraction from these samples was removed in a basic solution of Na_2CO_3 (1.5 N) at 85 °C for 5 h. The analyses on the opal- and carbonate-free fraction from respective drill sites were then performed on a Coulter LS-130 analyzer. For both ODP sites, sonication was not used to disaggregate the sediment dispersion, as previous measurements have shown that the use of ultrasonic dispersion could break brittle minerals (e.g., micas).

Spectral analysis on the mean sizes of siliciclastic grains from both ODP Sites 1144 and 1146 was performed using the Analyserie software (Paillard et al., 1996). The inversion algorithm for end-member modelling of compositional data (Weltje, 1997) has

been applied to the grain-size distributions of 291 and 726 samples from ODP Sites 1144 and 1146, respectively.

Terrigenous mass accumulation rates (MAR) ($\text{g}/\text{cm}^2/\text{kyr}$) were calculated using the following equations:

$$\text{MAR}_{\text{terrigenous}} = \text{MAR}_{\text{total}} - \text{MAR}_{\text{carbonated}}$$

$$\text{MAR}_{\text{terrigenous}} = [\text{Sed Rate}(\text{cm}/\text{kyr}) \times \text{Dry Density}(\text{g}/\text{cm}^3)] - (\text{MAR}_{\text{total}} \times \% \text{CaCO}_3)$$

Results

Siliciclastic grain size

The mean grain size of siliciclastic particles from both ODP Sites 1144 and 1146 varies mostly in the silt-size fraction and ranges between 6.8–38.8 μm and 4.1–23.8 μm , respectively (Fig. 2). Over the last 1.8 Ma, ODP Site 1146 downcore plots exhibit a two-stage evolution. Between 1.8 and 0.9 Ma, mean grain size is approximately 6.3 μm and does not show any major temporal variability. After 0.9 Ma, mean grain-size variations are similar at both sites and are characterized by large amplitudes variations in accordance with glacial/interglacial oscillations (Fig. 2B). Glacial stages are characterized, on average, by slightly coarser mean grain size than interglacial periods (Figs. 2A and B). Exceptions to this trend are noticeable during glacial Marine Isotope Stages 14, 18 and 20, which do not show significant increase of siliciclastic grain size.

Terrigenous mass accumulation rates calculated for ODP Sites 1144 and 1146 vary between 6–173 $\text{g}/\text{cm}^2/\text{kyr}$ and 4–27 $\text{g}/\text{cm}^2/\text{kyr}$, respectively. Even though the variations are not of the same order of magnitude between the two sites, the relative amplitude of shifts is similar (Fig. 2C). Low-amplitude terrigenous flux variations are recorded before 1 Ma but in younger intervals are well correlated with glacial/interglacial oscillations and terrigenous mass accumulation rates: almost every glacial stage is characterised by higher flux.

The power density spectrum reported in Figure 3 shows significant periodicities at ~ 100 kyr attributed to the eccentricity of the Earth's orbit, as well as unusual (non-Milankovitch-related) cycles at 76 and 65 kyr. However, this Blackman–Tukey method displays the periodicities of the entire record without taking account of their temporal evolution. Wavelet spectral analysis can decompose the record and helps to visualize the evolution through time of the periodicities. The results of this method are shown for the mean grain-size variations of both ODP sites in Figure 4. ODP Site 1146 wavelet analysis shows four major stages in the mean grain-size evolution: (i) from 1.8 to 1.25 Ma, no significant cyclicity is recorded, in accordance with the low changes of the mean grain size observed before 1.25 Ma (Fig. 2); (ii) from 1.25 to 0.9 Ma, a 100-kyr cycle gradually appears, (iii) from 0.9 to 0.35 Ma, the 100-kyr cycle increased and was strongly expressed after 0.6 Ma. This pattern is confirmed by the ODP Site 1144 wavelet analysis (Fig. 4). Additionally, periodicities at about 75 and 65 kyr are seen; and (iv) from 0.35 to 0 Ma, the only remaining periodicity is the 100-kyr cycle, recorded at both sites (Fig. 4).

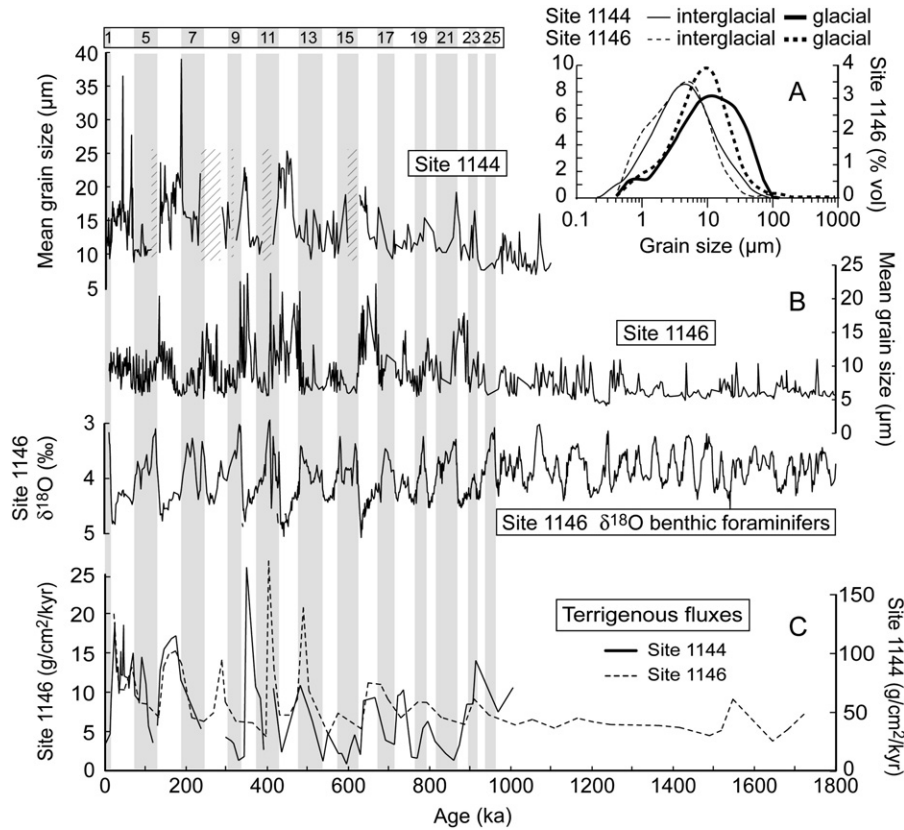


Figure 2. (A) Examples of glacial and interglacial grain-size distribution for both ODP Sites 1144 and 1146 showing glacial stages characterized by coarser grains. (B) Mean grain size variations of both ODP Sites 1144 and 1146 compared with benthic foraminifera (*U. Peregrina* and *C. Wuellerstorfi*) $\delta^{18}\text{O}$ curve over the last 1.8 Ma (Clemens and Prell, 2003; Buehring et al., 2004); dashed areas indicates hiatuses in the ODP Site 1144 sedimentation. (C) terrigenous mass accumulation rate variations for both ODP Sites 1144 and 1146 over the last 1.1 Ma and 1.8 Ma, respectively.

End-member modelling

The inversion algorithm for end-member modelling of compositional data display a three-end-member model that explains more than 90% of the variance (Fig. 5). The grain-size distributions of the three end-members (sub-populations) found at ODP Sites 1144 and 1146 are quite similar (Fig. 5). They are characterized by grain-size modes at 4, 9 and 19 μm for ODP Site 1146, and 5, 11, and 25 μm for ODP Site 1144.

For the last 1.8 Ma, the variation of the proportion of each sub-population suggests a three-stage evolution, with similar-

ities with those established for the mean grain-size variations and the wavelet analysis (Fig. 6). A first threshold occurs at 1.25 Ma, not observed on the mean grain-size variations but visible at ~ 1.2 Ma in the ODP Site 1146 wavelet analysis. Since 1.8 Ma, the fine end-member (4–5 μm) is dominant. It accounts for 72% of the average for the siliciclastic fraction and displays weak amplitude variations. The intermediate end-member (9–11 μm) content (mean value of 13%) variations are opposite from those of the fine end-member. The coarse end-member (19–25 μm) is quite low ($\sim 15\%$) and does not vary significantly with time (Fig. 6).

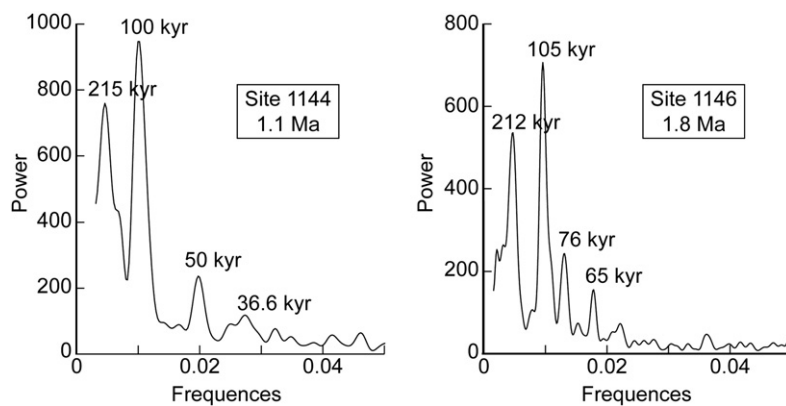


Figure 3. Spectral analyses of the mean grain-size record of both ODP Sites 1144 and 1146 over the last 1.1 Ma and 1.8 Ma, respectively.

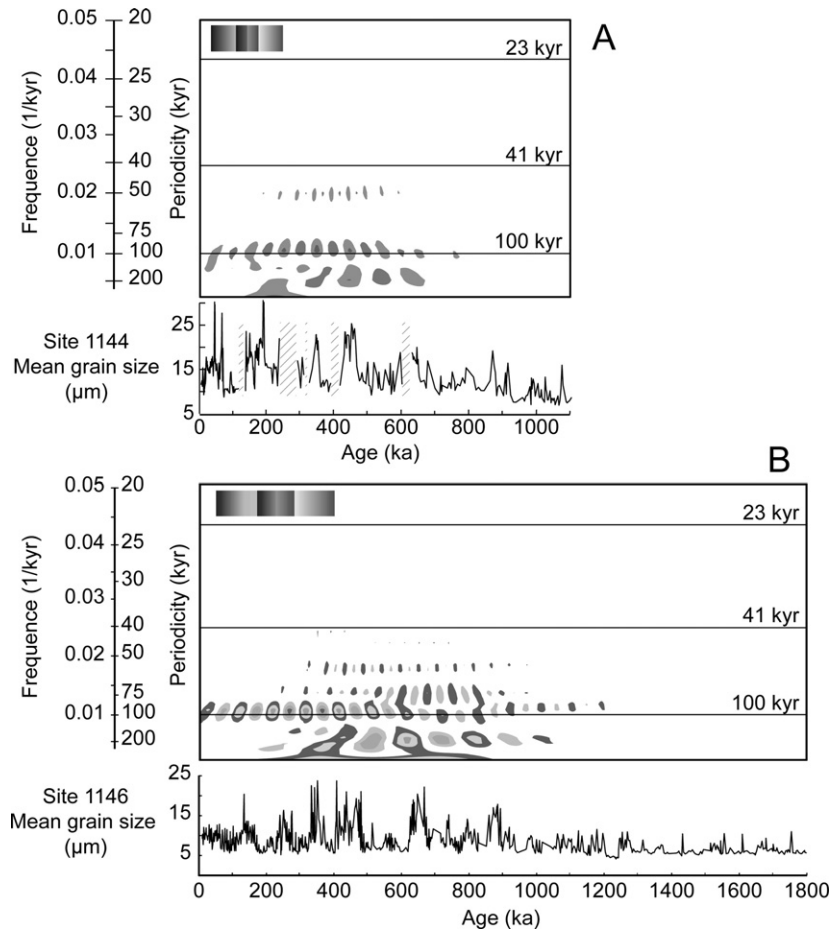


Figure 4. Wavelet spectral analyses of mean grain size for (A) ODP Site 1144 over 1.1 Ma and (B) ODP Site 1146 over 1.8 Ma.

From 1.25 to 0.9 Ma, both ODP sites are characterized by a major decrease of the relative abundance of the fine end-member, and an increase of the intermediate end-member

contribution. In contrast, the coarse end-member contribution remains constant with low values. Between 0.9 Ma and the present time, the coarse end-member content displays large-amplitude variations (2–75% and 4–63% respectively for ODP Sites 1144 and 1146) that are correlated with the glacial/interglacial oscillations. Apart from glacial Marine Isotope Stages 14, 16 and 18, abrupt increases in coarse end-member content characterize glacial stages.

Discussion

A re-evaluation of the eolian contribution to the South China Sea

Over the last million years, the mean grain-size, terrigenous mass accumulation rates and spectral analyses of both ODP Sites 1144 and 1146 indicate a strong glacial/interglacial response (Figs. 2–4), consistent with already published data, for the last 40 ka, of a core (17940) collected at the same position as ODP Site 1144 (Wang et al., 1999). The variations have been interpreted in terms of balance between fluvial (summer monsoon) and eolian (winter monsoon) input to the South China Sea (Wang et al., 1999). Studies on Chinese loess–paleosols sequences (e.g., An et al., 1990; Xiao et al., 1995; Heslop et al., 2000) and marine cores from the Northern Pacific

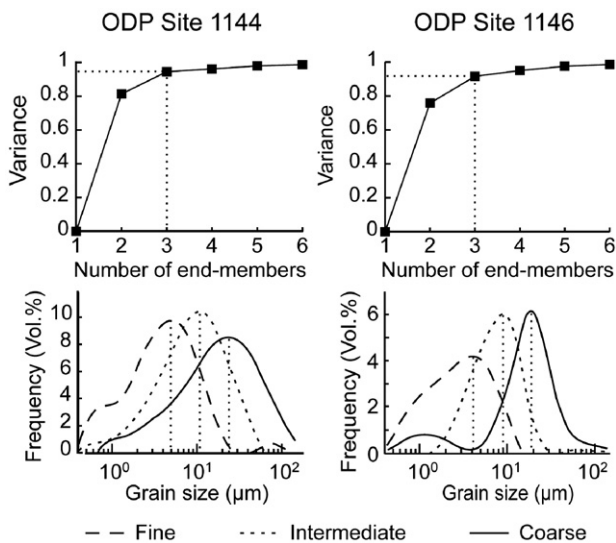


Figure 5. End-member modelling for ODP Sites 1144 and 1145. On the top part, the variance variations with different numbers of end-members, indicating that three end-members are enough to explain more than 90% of the variance. On the bottom part, the grain-size distribution obtained for a three-end-members model.

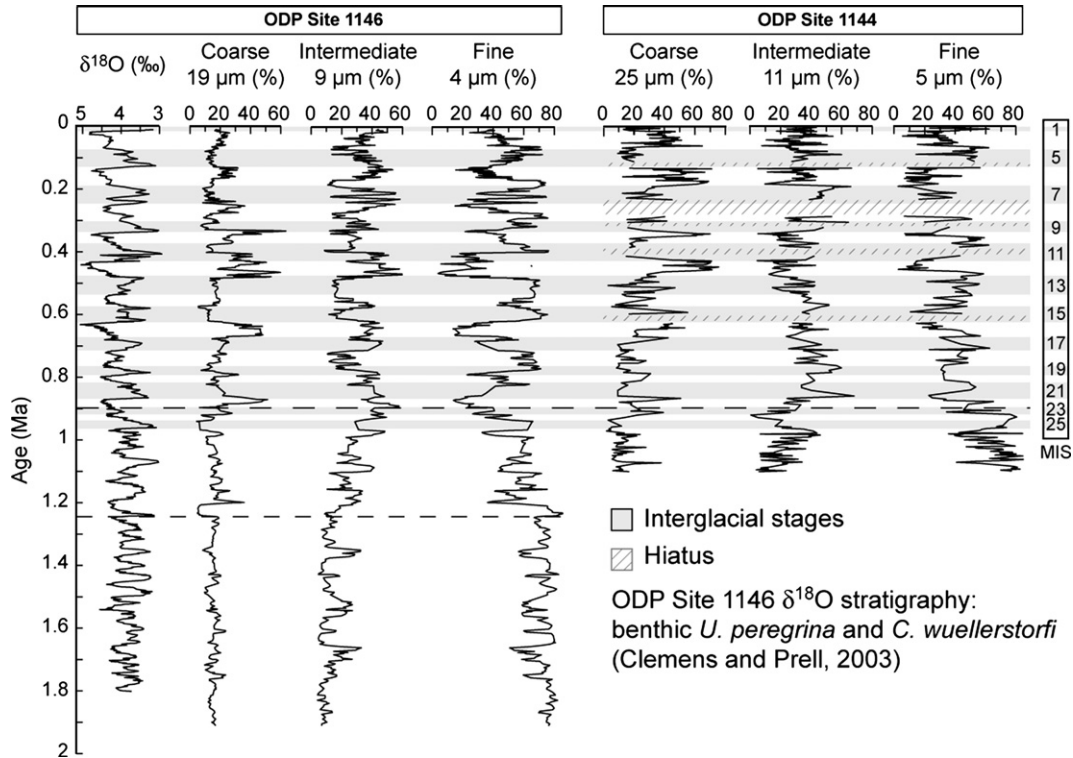


Figure 6. Relative abundances and variations of the 3 calculated end-members for the ODP Site 1146 over the last 1.8 Ma and the ODP Site 1144 over the last 1.1 Ma.

Ocean (e.g., Rea and Leinen, 1988; Rea and Hovan, 1995) confirm the dominant role of the jet streams for long-range transport of eolian particles during periods of strong winter monsoon.

End-member modelling of the grain-size data from ODP Sites 1144 and 1146 provides new insight into the source of siliciclastic sediments variations in the northern South China Sea. In the North Pacific, eolian particles average 8–15 μm in diameter close to the Japan East coast and around 1–10 μm in the North Pacific (e.g., Rea and Hovan, 1995). Considering the distance between the Loess Plateau and the South China Sea, the intermediate end-member (9–11 μm) could be consistent in size with this eolian population. However, its variability does not mirror the systematic increase observed during the glacial stages. Moreover, applying the eolian flux estimation of 50–100 $\text{g}/\text{cm}^2/\text{kyr}$ already used by Wehausen et al. (2003) for ODP Site 1145, and mean terrigenous fluxes of 76 $\text{g}/\text{cm}^2/\text{kyr}$ and 10 $\text{g}/\text{cm}^2/\text{kyr}$ calculated for ODP Sites 1144 and 1146, respectively, we calculate eolian flux contributions to the terrigenous fraction of 0.8–1.5% (Site 1144) and 5.5–11% (Site 1146). These results are not consistent with eolian supply, especially for the ODP Site 1144: ~1% of the terrigenous fraction cannot explain the huge mass accumulation rate and the variations of the grain-size parameters observed at this site.

Furthermore, over the last 2.6 Ma, loess–paleosols sequences in the Chinese Loess Plateau display a dominant glacial/interglacial variability with accumulation of coarser eolian particles during the arid glacial stages (e.g., Xiao and An, 1999; An, 2000; Heslop et al., 2000), but at ODP Site 1146, variations

of the mean grain size and end-member content are limited and do not correlate with glacial/interglacial changes before 1.25 Ma (Fig. 6), supporting an interpretation that these are separate phenomena.

All these arguments lead us to conclude that the eolian supply was a minor source of sediments. This hypothesis is supported by the fact that the South China Sea is located far south of the dominant atmospheric wind pathways that are responsible for the eolian dust transport. This circulation is mainly located between 30° and 45°N of latitude, where the upper tropospheric winds are most intense and enable the transport of eolian dust over long distances to the northern Pacific Ocean. We conclude that the grain-size record must be controlled by other processes.

ODP Sites 1144 and 1146 are located offshore (~500 km) of the modern Pearl River mouth (Fig. 1), which is one of the major fluvial sediment source to the South China Sea (present-day mean sediment discharge of $\sim 100 \times 10^6$ t/yr; Zhang et al., 1994). They were even closer to the paleo-river estuary (~250 km) during glacial stages when sea level was lower. Coupled with the mineralogical analyses, $^{87}\text{Sr}/^{86}\text{Sr}$ and $\epsilon\text{Nd}_{(0)}$ isotopes investigations conducted on sediment from ODP Site 1145 carbonate-free fraction are clearly located along a mixing curve linking the Pearl River and the volcanic Taiwan-Luzon Arc end-members. This confirms that the Pearl River is the main sedimentary source to the slope of the northern South China Sea (Boulay et al., 2005).

The shelf in front of the Pearl River mouth is shallow and wide (extends up to 300 km offshore). This implies that it is extremely sensitive to sea-level variations, but up until now,

sediment transport across the shelf has not been seriously considered as an explanation for observed grain-size variations in South China Sea sediments.

Unraveling global climate and the East Asian monsoon with grain-size record

Over the time interval 1.8–1.25 Ma, no relationship is observed between the $\delta^{18}\text{O}$ record of benthic foraminifera (Clemens and Prell, 2003) and the abundance of each of the three sub-populations. The first significant shift in both ODP Sites 1144 and 1146 grain-size records over the last 2 Ma appears at 1.25 Ma as an increase in the intermediate end-member content lasting until 0.9 Ma. This is in accordance with a major cooling period identified between 1.2 and 0.9 Ma in the northern hemisphere associated with an increase in sea-level variation amplitude between glacial and interglacial transitions (Berger and Jansen, 1994). Moreover, the coarse end-member begins to vary at 0.9 Ma, in accordance with the onset of strong glacial/interglacial oscillations observed in most of the world-wide paleoclimatic records and in the first major sea-level drop. It seems that the grain-size record is strongly correlated to the sea level.

During sea-level variations, several processes can be involved in the reworking of the shelf's sediment and its transport to the deep-water basin:

- (1) During high sea-level, the grain size on the shelf displays a progressive decreasing from the river mouth to the basin. The offshore migration of the shoreline and river mouth during glacial low sea level should be accompanied by a displacement of the granulometric zones, implying a coarsening at the site locations.
- (2) During sea-level lowstands, the hydrographic network tends to adapt to the new profile in order to reach its baseline. This causes a substantial erosion of the shelf, feeding the basin with coarser-grained material.
- (3) During these periods, the swell erodes mobile shelf sands initiating the formation of gullies, such as those found in the East China Sea (Berné et al., 2002). These can supply the basin with coarser sediment.

Prior to 0.9 Ma, sea-level variations in the South China Sea were probably not sufficient in magnitude to cause major changes in the basin morphology, and did not induce major reworking of the northern shelf sediments. After 0.9 Ma, glacial stages' sea-level falls were sufficient to subaerially expose much of the shelf, enabling sediment reworking as well as large-scale migration of the river mouth.

The long-term link between grain-size and sea-level variations is supported by the strong correlation between the ODP Site 1146 benthic foraminifera $\delta^{18}\text{O}$ record and the variability of the coarse sub-population (Fig. 6). The benthic $\delta^{18}\text{O}$ record can roughly be interpreted as representing polar ice volume variations. Sediment of glacial stages 10, 12, and 16 are characterized by large shifts of $\delta^{18}\text{O}$ corresponding to major sea-level falls. These stages are associated with a high content

of the coarse end-member (Fig. 6), as well as increased terrigenous mass accumulation rates (Fig. 2). In contrast, glacial Marine Isotope Stage 14, 18 and 20 are characterized by weaker shifts in the $\delta^{18}\text{O}$ record, smaller coarse end-member content, and low terrigenous mass accumulation rates.

However, reworking of the shelf deposits does not explain the variations of the fine and intermediate end-member contents observed in both ODP sites. In order to understand the behaviour of these two end-members, the fine/intermediate end-member ratio has been calculated and compared with the mineralogical smectite/(illite+chlorite) ratio (Liu et al., 2003; Trentesaux et al., 2003), the coarse fraction and the $\delta^{18}\text{O}$ variations (Clemens and Prell, 2003) (Fig. 7). This ratio enables us to eliminate the dilution that could be due to reworking on the shelf.

The clay mineralogy of the clay-size fraction indicates a glacial/interglacial cyclicity, with high illite, chlorite, and kaolinite content during glacial periods and high smectite content during interglacial periods (Liu et al., 2003; Trentesaux et al., 2003). Nevertheless, a higher temporal resolution study conducted on sediment from ODP Site 1145 over the last 450 ka indicates that smectite content variations depend on the intensity of the East Asian summer monsoon and display a strong 23-kyr cyclicity (Boulay et al., 2005). The earlier study suggested that the smectite/(illite+chlorite) ratio can be used as a proxy for the past evolution of the East Asian summer monsoon in the South China Sea, independent of the sea-level changes. When the summer monsoon is enhanced, the physical and chemical weathering of the volcanic rocks of the Taiwan-Luzon Arc produce huge amounts of smectite that is transported to the northern shelf of the South China Sea by dominant oceanic circulation associated with the summer monsoon intensification (Boulay et al., 2005).

$^{87}\text{Sr}/^{86}\text{Sr}$ and $\epsilon\text{Nd}_{(0)}$ isotopes measurements indicate that the contribution of the Taiwan-Luzon Arc to the northern margin of the South China Sea have varied between 3 and 15% of the lithic fraction (Boulay et al., 2005). The large distance between the volcanic arc and the ODP sites considered here implies that most of the sediment transported to the northern margin of the South China Sea is in the clay-size fraction. Such changes could not explain the magnitude variability observed in the fine end-member content (ranging between 5 and 90% of the siliciclastic fraction). Thus the grain size does not reflect variations in the sedimentary sources.

The fine and intermediate end-members' content variations seem to be more complicated than those observed in the coarse fraction, perhaps driven by multiple processes. Over the long term, the smectite/(illite+chlorite) ratio increased between 1.25 and 0.9 Ma and has been interpreted to reflect enhancement of the summer monsoon (Liu et al., 2003) that would have resulted in higher rainfalls and more chemical weathering over Southeast Asia. This is consistent with the progressive grain-size transition observed in the intermediate and fine end-members between 1.25 Ma and 0.9 Ma (Fig. 6). This increase in the coarser particles supply could be associated with a more efficient run-off due to the increasing rainfall. This hypothesis is supported by an increase in the

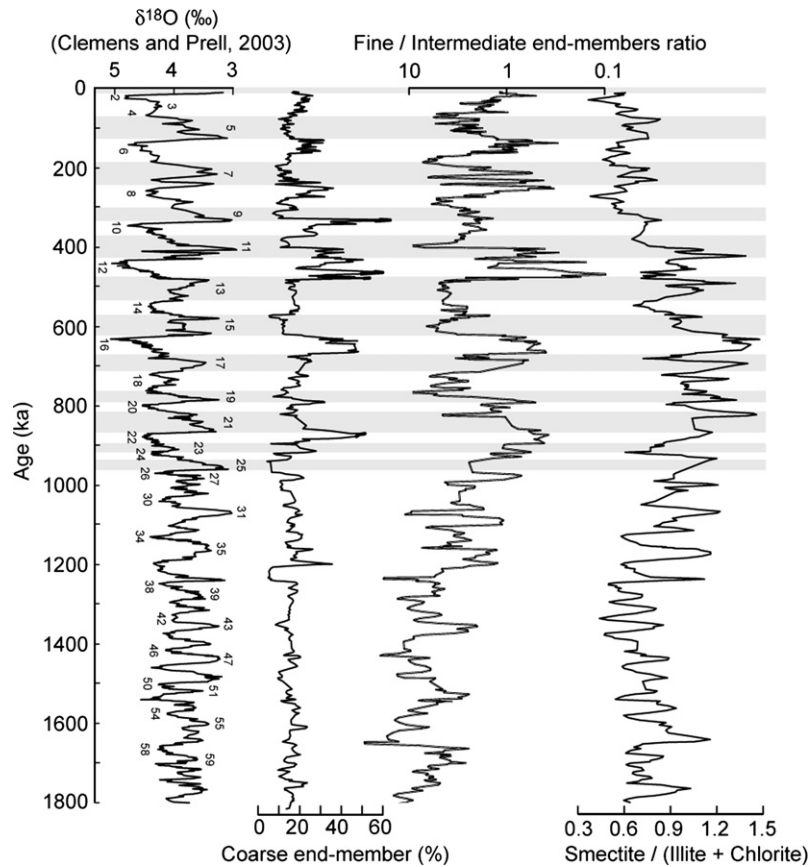


Figure 7. Coarse end-member, fine/intermediate end-member ratio and smectite/(illite+chlorite) ratio of the ODP Site 1146 over the last 1.8 Ma.

sedimentation rates in the South China Sea during this period (Jian et al., 2003). However, variations in sea level and the associated migration of the Pearl River mouth, which can transport more coarse particles to the basin, also have to be considered during this period. Specifically, there is a close relationship between the clay mineralogy and the fine/intermediate ratio between 1.8 and 0.9 Ma (Fig. 7). Periods of enhanced summer monsoon are characterized by high smectite/(illite+chlorite) ratio as well as high fine/intermediate end-member ratios. This indicates that when monsoon rainfall is enhanced, more fine-grained particles from the Pearl River are transported to the deep basin.

We suggest that the fine and intermediate-grained end-members do not respond to a single process but mirror the Pearl River's supply variations associated with rainfall and run-off changes over the Southeast Asian continent, as well as sea-level variations that induce changes in the geometry of the South China Sea and the location of the paleo-Pearl River mouth. Prior to 0.9 Ma, the fine/intermediate ratio essentially mirrors the pulses of fine particles transported by the Pearl River, with higher sediment inputs during East Asian summer monsoon intensity maxima. After 0.9 Ma, the grain-size ratio is affected by major reworking of the shelf and the variations of the coarse end-member. The relationship between siliclastic grain size and monsoon strength is less clear and it becomes difficult to separate the forcing due to the monsoon intensity from that due to paleogeographic variations.

An important decrease of the overall smectite/(illite+chlorite) trend at ODP Site 1146 occurs at about 400 ka, associated with a decrease in the amplitude of variations of the coarse population. For the last 450 ka, no relation between this ratio and the glacial/interglacial sea-level changes has been observed (Boulay et al., 2005). This is observed over the last 900 ka: strong glacial sea-level regressions that occurred during this period are not associated with smectite/(illite+chlorite) variations at ODP Sites 1145 and 1146. So, we suggest that the mineralogical decrease could simply reflect a weakening of the summer monsoon intensity, linked to strong glacial/interglacial oscillations taking place since ~600 ka in the high latitudes.

Mid-Pleistocene transition in the South China Sea

The South China Sea grain-size and clay-mineral variations presented here give new insight about global climatic changes occurring during the last 1.8 Ma and, especially, for the Mid-Pleistocene Transition. During this climatic transition, climate-induced responses to environmental change switched from a dominant 41-kyr cyclicality of obliquity towards a strong 100-kyr cyclicality of eccentricity, although orbital forcing of insolation did not change fundamentally (e.g., Pias and Moore, 1981; Imbrie et al., 1993). The timing of the Mid-Pleistocene Transition is documented by benthic foraminifera $\delta^{18}\text{O}$ records in marine sediments, indicating a general increase in global ice volume between ~1.2 and 0.9 Ma and the establishment of

strong 100-kyr cycles since 650 ka (e.g., Imbrie et al., 1993; Mudelsee and Schulz, 1997). We note that the origin of the Mid-Pleistocene Transition is still controversial, one of the key research goals at present being to understand whether the increase in mean global ice volume and the appearance of the ~100-kyr cycles are a response to, or the driver of, the Mid-Pleistocene climate change.

Most of Mid-Pleistocene Transition studies are based on foraminifer $\delta^{18}\text{O}$ or magnetic susceptibility data from deep-water hemipelagic sediments. The present study, using clay mineralogy and grain size patterns, adds low latitude “continental” evidence for major climatic change appearing much earlier than 0.9 Ma (the most commonly accepted threshold that marks the beginning of the Mid-Pleistocene Transition). This is in accordance with previous studies that demonstrated that the mechanism triggering this transition may include a tropical forcing (Rutherford and D’Hondt, 2000).

The increase of the smectite/(illite+chlorite) ratio after 1.25 Ma marks a reinforcement of Southeast Asian summer monsoon intensity. From then until ~0.9 Ma, Southeast Asia experienced enhanced rainfall and run-off. These continental climatic changes must be associated with an increase in the South China Sea surface temperature that could enhance atmospheric circulations, and thus evaporation and the moisture transport to the high latitudes. This is confirmed by several studies that show lighter benthic $\delta^{18}\text{O}$ values in the South China Sea between 1.2 and 0.9 Ma (Jian et al., 2003); while South China Sea waters, in connection with Pacific waters, decreased after 2.2 Ma (Jian et al., 2003). The South China Sea experienced a 300-kyr lightening of benthic foraminifera $\delta^{18}\text{O}$ that could indicate a warming of the deep-water temperature. Other evidence of sea-surface temperature changes include clues of a much warmer climate in the South China Sea area prior to 0.9 Ma (Zheng et al., 2005) and the magnification of the Walker circulation over the tropical Pacific that could increase the moisture transport to the high latitudes (de Garidel-Thoron et al., 2005; McClymont and Rosell-Melé, 2005). The possible deep-water temperature increase in the South China Sea is not consistent with sea-surface temperatures reconstructed in the western equatorial Pacific and that are stable over the Mid-Pleistocene Transition (de Garidel-Thoron et al., 2005; McClymont and Rosell-Melé, 2005). This could be due to the semi-enclosed basin morphology of the South China Sea. All the data presented here indicate that the sea level in the South China Sea and the Indo-Pacific adjacent area could have played an important role in that climatic transition.

Northern-hemisphere ice sheets experience a major expansion between 1.2 and 0.9 Ma that led to a reduced thermohaline circulation in the Atlantic Ocean and a mean global ice volume increase (e.g., Heinrich et al., 2002). This had a major impact on the paleogeography of the Indo-Pacific region, specifically of shallow sills that are highly sensitive to sea-level variations. From 1.25 Ma, the sea-level variations are of sufficient magnitude to reach depths of -40 m, which would close the main straits linking the South China Sea with the open ocean; the remaining link with the Pacific Ocean being the Luzon Strait, deeper than 2000 m.

Conclusions

From grain-size analyses and end-member modelling we have determined that the terrigenous fraction of the hemipelagic sediment from the northern part of the South China Sea is a mixture of three end-members with separate evolution over the last 1.8 Ma. The fine and intermediate sub-populations represent the flux of fluvial mud, which varies through time with the intensity of the summer monsoon and its associated rainfall, as well as with changes of the geometry of the South China Sea northern shelf and the movements of the Pearl River mouth. In contrast, the coarse population embodies the effect of sea-level variations over the shelf between glacial and interglacial stages (reflecting winnowing and seaward shifts of the Pearl River mouth).

Over the last 1.8 Ma, the grain-size record can be divided in three periods: (1) from 1.8 to 1.25 Ma, fine fluvial mud is dominant with no relation to sea-level changes but instead with the monsoon intensity; enhanced summer monsoon periods are characterized by heavy rainfall and associated with fine particles input that are eroded from surface soils and transported to the basin; (2) from 1.25 to 0.9 Ma, the fluvial input increases in concert with the coarsening fluvial grain-size that is associated with enhanced summer monsoon strength. The first appearance of significant variations of the coarse fraction of the sediment, as well as a slight increase of the intermediate end-member, indicates that sea-level variations started to impact the South China Sea shelf during this time; and (3) from 0.9 to 0 Ma, there is a good correlation between the grain-size record and glacial/interglacial oscillations, marked by coarse-grained input in the deep basin during the lowstands.

The South China Sea grain size and clay mineralogy indicate that the Mid-Pleistocene Transition could have a tropical origin. After 1.25 Ma, the first signs of an important climatic change are observed. Sea-level variations at this time are sufficient to almost close the Indo-Pacific water flow pathways, increasing the water temperature. The South China Sea, as a marginal sea, is highly sensitive to sea-level variations and when it is closed, its water can be easily warmed. As part of the Indo-Pacific Warm Pool, it could have played a role in the reinforcement of the atmospheric circulation and the Southeast Asian summer monsoon. The increase of moisture transfer from the ocean to the atmosphere, from low to high latitudes, could then have triggered or enhanced the 100-kyr ice-volume fluctuations as already demonstrated by Gildor and Tziperman (2000) and could explain the observed change at 1.25 Ma, from small thin to thick highly labile ice sheets that characterize the last million years.

Acknowledgments

This study is based on samples provided by the Ocean Drilling Program (ODP). ODP is sponsored by the U.S. National Science Foundation (NSF) and participating countries under management of Joint Oceanographic Institutions (JOI), Inc. Funding for this research was provided by the Centre National de la Recherche Scientifique (CNRS) with the French

Program OCEANS and ECLIPSE ASTRONOM, and by the AFCRST PRA 04-02, which permits positive collaboration between French and Chinese researchers. The authors gratefully acknowledge P. Clift and L. Giosan for their critical reviews and comments, as well as M. Allison for his careful reading of the manuscript.

References

- An, Z., 2000. The history and variability of the east Asian paleomonsoon climate. *Quaternary Science Reviews* 19, 171–187.
- An, Z., Liu, T., Lu, Y., Porter, S., Kukla, G., Wu, X., Hua, Y., 1990. The long-term paleomonsoon variation recorded by the loess–paleosoils sequence in central China. *Quaternary International* 7/8, 91–95.
- Beaufort, L., de Garidel-Thoron, T., Linsley, B., Oppo, D., Buchet, N., 2003. Biomass burning and oceanic primary production estimates in the Sulu Sea area over the last 380 kyr and the East Asian monsoon dynamics. *Marine Geology* 201, 53–65.
- Berger, W.H., Jansen, E., 1994. Mid-Pleistocene climate shift: the Nansen connection. In: Johannessen, O.M., Muensch, R.D., Overland, J.E. (Eds.), *The Role of the Polar Oceans in Shaping the Global Environment*. Geophysical Monography of the American Geophysical Union, vol. 85, pp. 295–311.
- Berné, S., Vagner, P., Guichard, F., Lericolais, G., Liu, Z., Trentesaux, A., Yin, P., Yi, H.I., 2002. Pleistocene forced regressions and tidal sand ridges in the East China Sea. *Marine Geology* 188, 293–315.
- Boulay, S., Colin, C., Trentesaux, A., Frank, N., Liu, Z., 2005. Sediment sources and East Asian monsoon intensity over the last 450 ky. Mineralogical and geochemical investigations on South China Sea sediments. *Palaeogeography, Palaeoclimatology, Palaeoecology* 228 (3–4), 260–270.
- Buehring, C., Sarnthein, M., Erlenkeuser, H., 2004. Toward a high-resolution stable isotope stratigraphy of the last 1.1 m.y.: site 1144, South China Sea. In: Prell, W., Wang, P., Blum, P., Rea, D., Clemens, S. (Eds.), *Proc. ODP, Sci. Results*, p. 184 ([Online]. Available from World Wide Web: http://www-odp.tamu.edu/publications/184_SR/205/205.htm).
- Clemens, S., Prell, W., 2003. Data report: oxygen and carbon isotopes from Site 1146, northern South China Sea. In: Prell, W., Wang, P., Blum, P., Rea, D., Clemens, S. (Eds.), *Proc. ODP, Sci. Results*, p. 184 ([Online]. Available from World Wide Web: http://www-odp.tamu.edu/publications/184_SR/214/214.htm).
- Clemens, S., Prell, W., Murray, D., Shimmield, G., Weedon, G., 1991. Forcing mechanisms of the Indian Ocean Monsoon. *Nature* 353, 720–725.
- Clift, P., 2006. Controls on the erosion of Cenozoic Asia and the flux of clastic sediment to the ocean. *Earth and Planetary Science Letters* 241 (3–4), 571–580.
- Colin, C., Kissel, C., Blamart, D., Turpin, L., 1998. Magnetic properties of sediments in the Bay of Bengal and the Andaman Sea: impact of rapid North Atlantic Ocean climatic events on the strength of the Indian monsoon. *Earth and Planetary Science Letters* 160, 623–635.
- Colin, C., Turpin, L., Bertaux, J., Desprairies, A., Kissel, C., 1999. Erosional history of the Himalayan and Burman ranges during the last two glacial–interglacial cycles. *Earth and Planetary Science Letters* 171, 647–660.
- de Garidel-Thoron, T., Rosenthal, Y., Bassinot, F., Beaufort, L., 2005. Stable sea surface temperature in the western Pacific warm pool over the past 1.75 million years. *Nature* 433, 294–298.
- Ding, Z., Liu, T.-S., Rutter, N., Yu, Z., Guo, Z.-T., Zhu, R., 1995. Ice-volume Forcing of East Asian Winter Monsoon Variations in the Past 800,000 years. *Quaternary Research* 44, 149–159.
- Gildor, H., Tziperman, E., 2000. Sea ice as the glacial cycles' climate switch: role of seasonal and orbital forcing. *Paleoceanography* 15, 605–615.
- Heinrich, R., Baumann, K.-H., Huber, R., Meggers, H., 2002. Carbonate preservation records of the past 3 Myr in the Norwegian-Greenland Sea and the northern North Atlantic: implications for the history of NADW production. *Marine Geology* 184, 17–39.
- Heslop, D., Langereis, C., Dekkers, M., 2000. A new astronomical timescale for the loess deposits of Northern China. *Earth and Planetary Science Letters* 184, 125–139.
- Imbrie, J., Berger, A., Boyle, E., et al., 1993. On the structure and origin of major glaciation cycles. 2. The 100,000-year cycle. *Paleoceanography* 8, 699–735.
- Jian, Z., Huang, B., Kuhnt, W., Lin, H.-L., 2001. Late Quaternary upwelling intensity and East Asian monsoon forcing in the South China Sea. *Quaternary Research* 55, 363–370.
- Jian, Z., Zhao, Q., Cheng, X., Wang, J., Wang, P., Su, X., 2003. Pliocene–Pleistocene stable isotope and paleoceanographic changes in the northern South China Sea. *Palaeogeography, Palaeoclimatology, Palaeoecology* 193 (3–4), 425–442.
- Liu, Z., Trentesaux, A., Clemens, S., Colin, C., Wang, P., Huang, B., Boulay, S., 2003. Clay mineral assemblages in the northern South China Sea: implications for East Asian monsoon evolution over the past 2 million years. *Marine Geology* 201, 133–146.
- McClymont, E., Rosell-Melé, A., 2005. Links between the onset of modern Walker circulation and the mid-Pleistocene climate transition. *Geology* 33 (5), 389–392.
- Mudelsee, M., Schulz, M., 1997. The Mid-Pleistocene climate transition: onset of 100 ka cycle lags ice volume build-up by 280 ka. *Earth and Planetary Science Letters* 151, 117–123.
- Paillard, D., Labeyrie, L., Yiou, P., 1996. Analyseries 1.0: a Macintosh software for the analysis of geographical time-series. *EOS* 77, 123–152.
- Pisias, N., Moore, T., 1981. The evolution of Pleistocene climate: a time series approach. *Earth and Planetary Science Letters* 52, 450–458.
- Prins, M.A., Weltje, G.J., 1999. End-member modeling of siliciclastic grain-size distributions: The late Quaternary record of eolian and fluvial sediment supply to the Arabian Sea and its paleoclimatic significance. In: Harbaugh, J., et al. (Eds.), *Numerical Experiments in Stratigraphy: Recent Advances in Stratigraphic and Sedimentologic Computer Simulations*. SEPM (Society for Sedimentary Geology) Special Publication., vol. 62, pp. 91–111.
- Prins, M., Postma, G., Cleveringa, J., Cramp, A., Kenyon, N., 2000. Controls on terrigenous sediment supply to the Arabian Sea during the late Quaternary: the Indus Fan. *Marine Geology* 169, 327–349.
- Rea, D., Hovan, S., 1995. Grain-size distribution and depositional processes of the mineral component of abyssal sediments: lessons from the North Pacific. *Paleoceanography* 10, 251–258.
- Rea, D., Leinen, M., 1988. Asian aridity and the zonal westerlies: Late Pleistocene and Holocene record of eolina deposition in the northwest Pacific Ocean. *Palaeogeography, Palaeoclimatology, Palaeoecology* 66, 1–8.
- Rutherford, S., D'Hondt, S., 2000. Early onset and tropical forcing of 100,000 year Pleistocene glacial cycles. *Nature* 408, 72–74.
- Sun, X., Luo, Y., Huang, F., Tian, J., Wang, P., 2003. Deep-sea pollen from the South China Sea: Pleistocene indicators of East Asian monsoon. *Marine Geology* 201, 97–118.
- Tamburini, F., Adatte, T., Föllmi, K., Bernasconi, S., Steinmann, P., 2003. Investigating the History of East Asian monsoon and climate during the last glacial interglacial period (0–140,000 years): mineralogy and geochemistry of ODP Site 1143 and 1144, South China Sea. *Marine Geology* 201, 147–168.
- Trentesaux, A., Liu, Z., Colin, C., Boulay, S., Wang, P., 2003. Data report: Pleistocene paleoclimatic cyclicity of southern China: clay mineral evidence recorded in the South China Sea (ODP Site 1146). In: Prell, W., Wang, P., Blum, P., Rea, D., Clemens, S. (Eds.), *Proc. ODP, Sci. Results*, p. 184 ([Online]. Available from World Wide Web: http://www-odp.tamu.edu/publications/184_SR/210/210.htm).
- Wang, L., Sarnthein, M., Erlenkeuser, H., Grimalt, J., Grootes, P., Heilig, S., Ivanova, E., Kienast, M., Pelejero, C., Pflaumann, U., 1999. East Asian monsoon climate during the Late Pleistocene: high-resolution sediment records from the South China Sea. *Marine Geology* 156, 245–284.
- Webster, P., 1987. *The Elementary Monsoon*. John Wiley & Sons, New York, pp. 3–32.
- Wehausen, R., Brumsack, H.-J., 2002. Astronomical forcing of the East Asian monsoon mirrored by the composition of Pliocene South China Sea sediments. *Earth and Planetary Science Letters* 201, 621–636.
- Wehausen, R., Tian, J., Brumsack, H.-J., Cheng, X., Wang, P., 2003. Geochemistry of Pliocene sediments from ODP Site 1143 (southern South China Sea). In: Prell, W., Wang, P., Blum, P., Rea, D., Clemens,

- S. (Eds.), Proc. ODP, Sci. Results, p. 184 ([Online]. Available from World Wide Web: http://www-odp.tamu.edu/publications/184_SR/201/201.htm).
- Wei, G., Liu, Y., Li, X.-H., Shao, L., Fang, D., 2004. Major and trace element variations of the sediments at ODP Site 1144, South China Sea, during the last 230 ka and their paleoclimate implications. *Palaeogeography, Palaeoclimatology, Palaeoecology* 212 (3–4), 331–342.
- Weltje, G., 1997. End-member modelling of compositional data: numerical-statistical algorithms for solving the explicit mixing problem. *Journal of Mathematical Geology* 29, 503–549.
- Xiao, J., An, Z., 1999. Three large shifts in East Asian monsoon circulation indicated by loess–paleosol sequences in China and late Cenozoic deposits in Japan. *Palaeogeography, Palaeoclimatology, Palaeoecology* 154, 179–189.
- Xiao, J., Porter, S., An, Z., Kumai, H., Yoshikawa, S., 1995. Grain size of quartz as an indicator of winter monsoon strength on the loess plateau of central China during the last 130,000 yr. *Quaternary Research* 43, 22–29.
- Zhang, J., Huang, W., Liu, M., 1994. Geochemistry of major Chinese river-estuary systems. In: Zhou, D., et al. (Eds.), *Oceanology of China Seas*, vol. 1. Kluwer Academic, Dordrecht, pp. 179–188.
- Zheng, F., Li, Q., Li, B., Chen, M., Tu, X., Tian, J., Jian, Z., 2005. A millennial scale planktonic foraminifer record of the mid-Pleistocene climate transition from the northern South China Sea. *Palaeogeography, Palaeoclimatology, Palaeoecology* 223, 349–363.